

Interplay of Self-Association and Solvation in Polar Liquids

Valeria Amenta,[†] Joanne L. Cook,[†] Christopher A. Hunter,^{*,†} Caroline M. R. Low,[‡] Hongmei Sun,[†] and Jeremy G. Vinter[§]

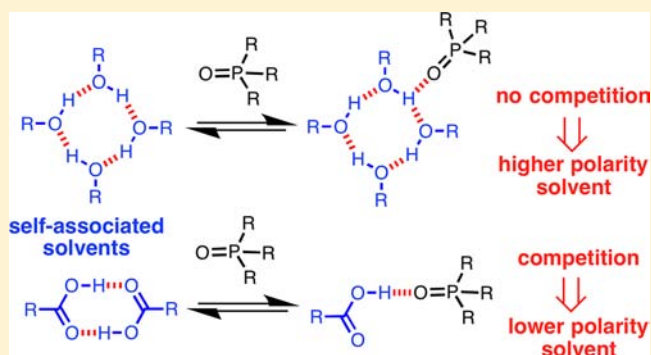
[†]Department of Chemistry, University of Sheffield, Sheffield, S3 7HF United Kingdom

[‡]Drug Discovery Facility, Room 512 Biochemistry, Imperial College, London SW7 2AY United Kingdom

[§]Cresset Biomolecular Discovery, BioPark Hertfordshire, Broadwater Road, Welwyn Garden City AL7 3AX United Kingdom

Supporting Information

ABSTRACT: The association constants for formation a 1:1 complex between 4-phenyl azophenol and tri-*n*-butylphosphine oxide were measured in mixtures of *n*-octane and *n*-decanol, *n*-octane and *n*-hexanoic acid, and *n*-octane and 2-ethylhexyl acetamide. The experiments provide insight into the competition between solvent self-association and solvent–solute interactions in these systems. The solvation properties of the three polar solvents are quite different from one another and from polar solvents that do not self-associate. Carboxylic acids form dimers in concentrated solution (>1 mM in alkanes). Carboxylic acid dimers have exposed H-bond acceptor sites that solvate H-bond donor solutes with a similar binding affinity to carboxylic acid monomers. The carboxylic acid H-bond donor site is inaccessible in the dimer and is not available to solvate H-bond acceptor solutes. The result is that solvation of H-bond acceptor solutes is in competition with solvent dimerization, whereas solvation of H-bond donor solutes is not. Secondary amides form linear polymers in concentrated solution (>10 mM in alkanes). The solvation properties of the secondary amide aggregates are similar to those of carboxylic acid dimers. Solvation of H-bond acceptor solutes must compete with solvent self-association, because the amide H-bond donor site is not accessible in the middle of a polymeric aggregate. However, the amide aggregates have exposed H-bond acceptor sites, which solvate H-bond donor solutes with similar binding affinity to amide monomers. Alcohols form cyclic tetramers at concentrations of 100 mM in alkanes, and these cyclic aggregates are in equilibrium with linear polymeric aggregates at concentrations above 1 M. The alcohol aggregates have exposed H-bond acceptor sites that solvate H-bond donor solutes with similar binding affinity to alcohol monomers. Although the alcohol H-bond donor sites are involved in H-bond interactions with other alcohols in the aggregates, these sites are sufficiently exposed to form a second bifurcated H-bond with H-bond acceptor solutes, and these interactions have a similar binding affinity to alcohol monomers. The result is that self-association of alcohols does not compete with solvation of solutes, and alcohols are significantly more polar solvents than expected based on the properties of alcohol monomers.



INTRODUCTION

The relationship between solute and solvent plays a critical role in a wide range of chemical processes.^{1,2} However, the solution phase is a complex system, where the solvation environment of a molecule is determined by the interplay of many different pairwise intermolecular interactions and cooperative assembly processes.^{3,4} Structural information can only be obtained by indirect spectroscopic methods or from molecular simulation techniques, which are still at a stage where it is difficult to make reliable quantitative predictions.^{5–13} Thermodynamic measurements report on the properties of the system as a whole, which makes it difficult to disentangle the many different contributions that determine the overall properties of a solution. We have shown that H-bonded complexes can be used to probe the properties of a specific site in the solvation shell of a solute.^{14–16} This is much simpler than understanding the entire solvation shell and allows direct quantification of the

competition between specific solvent–solvent and solvent–solute interactions. Here we apply this approach to investigate the role of solvent self-association in determining the solvation properties of polar liquids, such as alcohols, carboxylic acids, and secondary amides.

Carboxylic acids self-associate to form dimers held together by two cooperative H-bonding interactions (Figure 1a).¹⁷ Competition between this dimerization process and interactions with solutes plays an important role in determining the solvation properties of these solvents.¹⁸ The predominant mode of self-association of secondary amides is formation of open chain polymers via single H-bonding interactions (Figure 1b).^{19–25} The difference between amides and carboxylic acids is related to differences in the preferred conformations of the

Received: June 10, 2013

Published: August 5, 2013

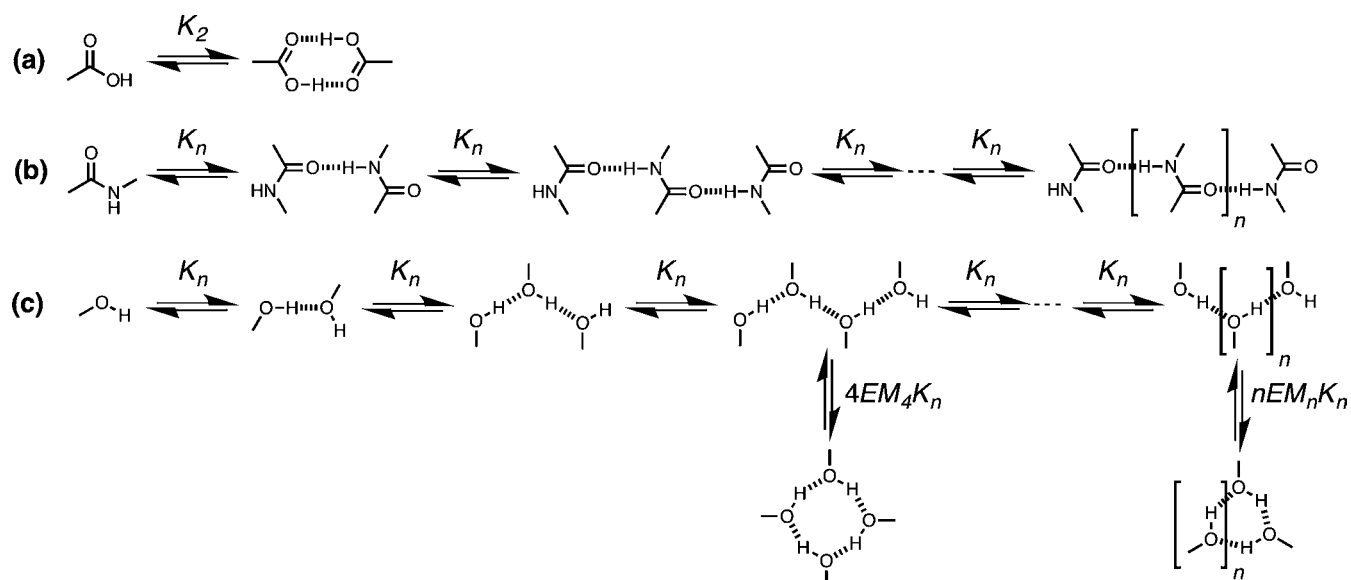


Figure 1. Self-association of polar solvents. (a) Carboxylic acids form dimers with a self-association constant K_2 . (b) Amides form linear polymers with a stepwise self-association constant K_n . (c) Alcohols form linear and cyclic oligomers as well as polymers. K_n is the self-association constant for isodesmic polymerization, and EM_n is the effective molarity for intramolecular cyclization of a linear n -mer.

functional groups. In carboxylic acids, the carbonyl acceptor and H-bond donor are arranged in a *cis* orientation, whereas in secondary amides they are usually *trans*.

The self-association of alcohols is more complicated involving both closed cyclic and open polymeric aggregates (Figure 1c).^{26–29} A study of the interaction of alcohols with pyridine N-oxide in cyclohexane suggested that alcohol aggregates interact more strongly with solutes than the corresponding monomers.³⁰ We measured the stability of the H-bonded complex formed by perfluoro-*t*-butyl alcohol and tri-*n*-butylphosphine oxide in 13 different solvents. Equation 1 accurately predicted the association constants for all solvents with the exception of *n*-decanol, which was the only strongly self-associating solvent used in this study.³¹ The values of α_S and β_S used in eq 1 were measured for monomeric alcohols in dilute solution, and the experimental association constant in *n*-decanol is more than an order of magnitude lower than eq 1 predicts. This suggests that the bulk liquid is significantly more polar than alcohol monomers.

$$-RT \ln K = -(\alpha - \alpha_S)(\beta - \beta_S) + 6 \text{ kJ mol}^{-1} \quad (1)$$

where α and β are the H-bond parameters of the solutes and α_S and β_S are corresponding H-bond parameters of the solvent.

Abraham recently measured association constants for a series of H-bonded complexes in *n*-octanol using headspace gas liquid chromatography.³² The experimental association constants were generally an order of magnitude higher than predicted by eq 1. These results suggest that the bulk liquid is significantly less polar than expected based on the properties of alcohol monomers. In an effort to rationalize these contradictory results and understand the solvation properties of self-associating solvents, we describe here the use of a molecular recognition probe to quantify solvent–solute interactions in mixtures of alkanes with carboxylic acids, secondary amides, and alcohols.

The H-bonded complex formed between 4-phenyl azophenol (D) and tri-*n*-butylphosphine oxide (A) provides a convenient probe that we have previously used to investigate the properties

of solvent mixtures (Figure 2).^{14–16} Figure 3 shows that two different solutes (A and D) dissolved in a mixture of two

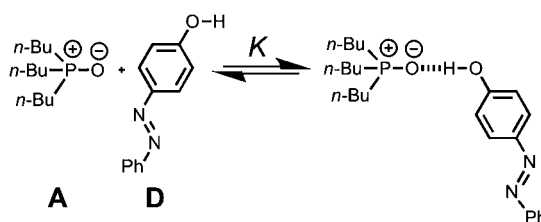


Figure 2. Formation of a 1:1 complex between a H-bond donor (D) and a H-bond acceptor (A) with an association constant K .

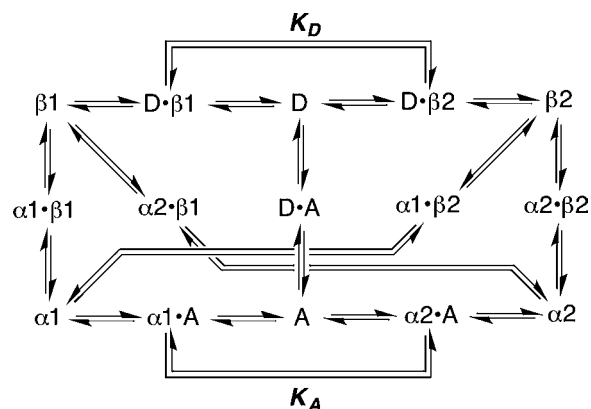


Figure 3. Equilibria present for two different solutes, A and D, dissolved in a mixture of two different solvents, S1 and S2. The species D, A represent unsolvated states of the solutes, and α_1 , α_2 , β_1 , and β_2 represent unsolvated states of the solvent H-bond donor and acceptor sites. K_A and K_D are, respectively, the A-S2 and D-S2 association constants in S1.

different solvents (S1 and S2) leads to a large number of different solvation states that influence the overall equilibrium constant for formation of the A-D complex (K). Therefore measurement of the A-D association constant as a function of

solvent composition provides quantitative information on the solvation equilibria present in these systems.

To date, we have focused on mixtures of a very nonpolar solvent (*n*-octane as S1) and a more polar solvent (S2), which contains either a H-bond donor or a H-bond acceptor site, but not both (e.g., di-*n*-hexyl ether). In other words, S2 is a polar solvent that does not self-associate to any significant extent. Under these conditions, the solvent–solvent interactions are approximately independent of the solvent composition, and one of the two equilibria highlighted as K_D and K_A in Figure 3 dominates the solvation properties of the system. The results for these solvent systems are illustrated schematically in Figure 4.

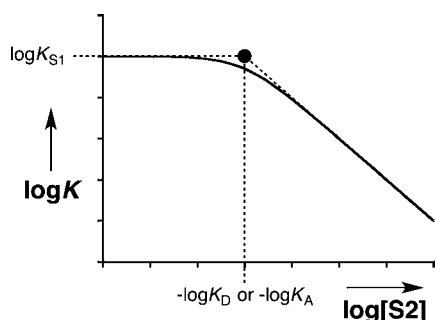


Figure 4. Solvent dependence of the association constant, $\log K$, for formation of a H-bonded complex, D·A, in mixtures of a nonpolar solvent, S1, and a polar solvent, S2, where S2 does not self-associate to a significant extent. The position of the horizontal dashed line is defined by the 1:1 association constant for formation of the D·A complex in S1 (K_{S1}), which depends on the polarity of D, A, and S1 but is independent of S2. The position of the vertical dashed line is defined by the 1:1 association constant for formation of the D·S2 complex in S1 (K_D) or for formation of the A·S2 complex in S1 (K_A).

The $\log K$ versus $\log[S2]$ profile shows a region where the A·D association constant is invariant with solvent composition (slope ≈ 0), then as the concentration of solvent S2 in the mixture increases, the association constant for the A·D complex starts to decrease. In this region, the gradient of the profile is -1 . This gradient implies that a 1:1 interaction between S2 and one of the two solutes competes with formation of the A·D complex. This was confirmed by independently measuring the values of K_D and K_A , the association constants for formation of the S2·D and S2·A complexes in an S1 solvent. The association constant for the most stable S2:solute complex (K_D or K_A) provides a good indicator of the point at which the gradient in the $\log K$ versus $\log[S2]$ profile in Figure 4 changes.

In this paper, we apply this experiment to solvents that contain both strong H-bond donor and acceptor sites, carboxylic acids, secondary amides, and alcohols. For these systems, all of the equilibria shown in Figure 3 become important, and consequently the form of the $\log K$ versus $\log[S2]$ profile can provide insight into the role of self-association in determining the solvation properties of polar solvents.

RESULTS AND DISCUSSION

Association constants for formation of 1:1 H-bonded complexes between D and A were measured in *n*-octane/*n*-decanol, *n*-octane/*n*-hexanoic acid, and *n*-octane/2-ethylhexyl acetamide mixtures using high-throughput UV–vis titration experiments. *n*-Decanol and *n*-hexanoic acid are commercially

available. 2-Ethylhexyl acetamide was synthesized from 2-ethylhexylamine and acetyl chloride. This amide was used to ensure good miscibility with *n*-octane.

Before discussing the results obtained for these four component systems, we will consider the properties of the two component system, S1–S2, and the three components systems, S1–A–D, S1–S2–A and S1–S2–D, which allow independent characterization of some the equilibria shown in Figure 3. ^1H NMR spectra in *n*-octane were complicated by signal overlap, and cyclohexane was therefore used as S1 for some of these experiments. To determine whether changing the nature of the alkane used as S1 has a significant effect on the equilibria, we investigated the effect of different alkanes on the association constant for formation of the A·D complex in the S1–A–D three component system.

Solvation Properties of Alkanes. UV–vis absorption titrations were used to measure the association constant for formation of the A·D complex, K , in eight different alkanes: *n*-octane, *n*-hexane, *n*-decane, *n*-dodecane, *n*-tetradecane, cyclopentane, cyclohexane, and *cis*-decalin. The absorption maximum of D occurs between 336 and 339 nm depending on the solvent, and addition of A leads to the appearance of a new absorption band due to the A·D complex at 356 nm.¹⁵ The titration data fit well to a 1:1 binding isotherm in all cases, and the results are reported in Table 1. The association constants

Table 1. Association Constants (K , M^{-1}) for Formation of the A·D Complex Measured by UV–vis Absorption Titrations in Alkanes at 295 K^a

solvent	K	$\log K$
<i>n</i> -hexane	$6.2 \pm 0.1 \times 10^4$	4.8 ± 0.2
<i>n</i> -octane	$7.4 \pm 0.1 \times 10^4$	4.9 ± 0.1
<i>n</i> -decane	$1.2 \pm 0.3 \times 10^5$	5.1 ± 0.2
<i>n</i> -dodecane	$8.2 \pm 0.8 \times 10^4$	4.9 ± 0.1
<i>n</i> -tetradecane	$6.3 \pm 0.3 \times 10^4$	4.8 ± 0.1
cyclopentane	$1.1 \pm 0.1 \times 10^5$	5.0 ± 0.1
cyclohexane	$1.6 \pm 0.1 \times 10^5$	5.2 ± 0.1
<i>cis</i> -decalin	$9 \pm 4 \times 10^4$	4.9 ± 0.4

^aAll experiments were repeated at least twice, and average values are quoted. The errors in K are twice the standard deviation.

do not vary significantly with the nature of the alkane, and $\log K/\text{M}^{-1}$ is 5.0 ± 0.2 in all cases. We conclude that the solvation properties of different alkanes are similar, at least with respect to solute interactions and that data measured in cyclohexane and in *n*-octane can be reasonably compared.

Self-Association of Polar Solvents in Alkanes. ^1H NMR dilution experiments were used to investigate self-association of the three polar solvents (S2) in *d*₁₂-cyclohexane (S1). The data for *n*-hexanoic acid fit well to a simple dimerization isotherm (Figure 1a) giving a self-association constant $K_2 = 1100 \pm 100 \text{ M}^{-1}$.¹⁷ The data for 2-ethylhexyl acetamide fit well to an isodesmic polymerization isotherm (Figure 1b) giving a self-association constant $K_n = 140 \pm 20 \text{ M}^{-1}$.^{19,33}

The situation is more complicated for *n*-decanol. Changes in the chemical shifts of the signals due to the OH and $\alpha\text{-CH}_2$ protons were monitored as a function of concentration. The dilution data do not fit well to either the simple dimerization or isodesmic polymerization isotherms used to analyze self-association of the acid and amide (Figure 5a,b). The data were therefore fit to more complicated isotherms that allow for the presence of closed cyclic as well as open linear oligomers

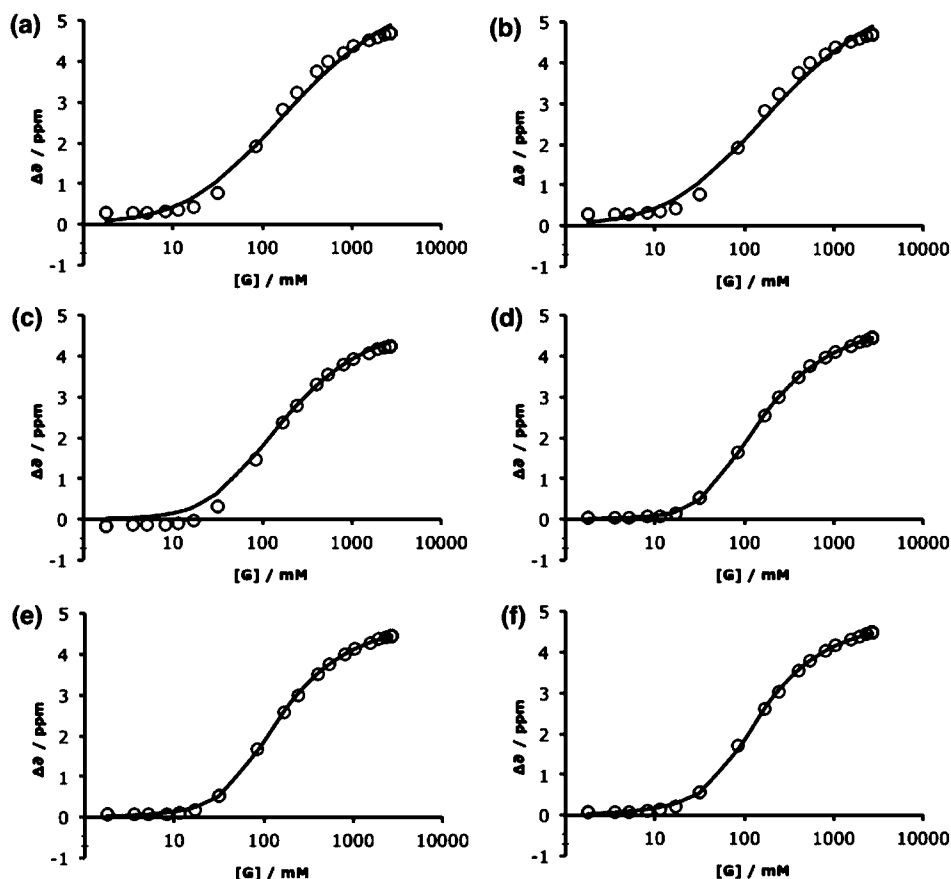


Figure 5. ^1H NMR data for dilution of *n*-decanol in d_{12} -cyclohexane at 295 K. The data points show the change in chemical shift of the signal due to the OH proton, and the lines are the best fit to (a) isodesmic polymerization (error in fit 6.0%), (b) dimer (error in fit 6.0%), (c) trimer plus polymer (error in fit 6.0%), (d) tetramer plus polymer (error in fit 0.6%), (e) pentamer plus polymer (error in fit 0.9%), (f) hexamer plus polymer (error in fit 1.3%) isotherms.

(Figure 1c).³⁴ The results are shown in Figure 5, and the best fit was obtained for a tetramer plus polymer isotherm (Figure 5d) giving the macroscopic association constant $K_4 = 4 \text{ EM}_4 K_n = 820 \text{ M}^{-3}$ for formation of the cyclic tetramer (see Figure 1c) and the stepwise association constant $K_n = 2 \text{ M}^{-1}$ for isodesmic polymerization.

The *n*-decanol ^1H NMR dilution data also fit reasonably well to models that include formation of cyclic pentamers or cyclic hexamers in addition to the open polymer (Figure 5e,f). In reality, there are probably mixtures of different cyclic oligomers present, but the tetramer predominates at low concentrations, because it is entropically favored over larger oligomers. However, there is crystallographic evidence suggesting that alcohols prefer to self-associate as cyclic tetramers. An analysis of the crystal structures of alcohols in the Cambridge Structural Database showed that linear and cyclic H-bonded aggregates are equally populated, but three-quarters of the cyclic structures are tetrameric.³⁵ The preference for the formation of cyclic tetramers means that monoalcohols are five times more likely to crystallize in a tetragonal or trigonal space group than other molecules. Figure 6 shows some examples of alcohol cyclic tetramer motifs found in the CSD. Evidence for the preference of alcohols to form tetramers also comes from the concentration dependence of the apparent molar heat capacities of alcohol/alkane mixtures.²⁸

The relative proportions of the two different oligomeric forms of *n*-decanol are different at different concentrations, and this should affect the solvation properties of alcohol/alkane

mixtures. Comparison of the values of K_4 and K_n allows estimation of the concentration of *n*-decanol at which the closed cyclic tetramer opens up to form the open linear polymer, EM_4 (Figure 1c, eq 2). However, the NMR experiment is not sensitive to this equilibrium, and so the value of K_n determined in the NMR dilution experiment is subject to a large error (<12% of species are present as open polymer according to the fit shown in Figure 5e).

$$\text{EM}_4 = \frac{K_4}{4K_n^4} \quad (2)$$

In contrast, viscosity is insensitive to the formation of small cyclic oligomers but very sensitive to the formation of large linear polymers. Viscosity data from the literature for *n*-decanol/*n*-heptane mixtures are shown in Figure 7: the relative viscosity of the mixture, η_{rel} , as defined in eq 3, is plotted as a function of the logarithm of the concentration of alcohol, $\log[S_2]$.³⁶

$$\eta_{\text{rel}} = \frac{\eta - \eta_{S_1}}{\eta_{S_2} - \eta_{S_1}} \quad (3)$$

where η is the viscosity of the mixture, η_{S_1} is the viscosity of pure *n*-heptane, and η_{S_2} is the viscosity of pure *n*-decanol.

There is a large increase in viscosity when the concentration of *n*-decanol increases above 1 M. The onset of the viscosity increase can be compared with the speciation of different oligomers based on the NMR dilution data. Figure 7 shows that

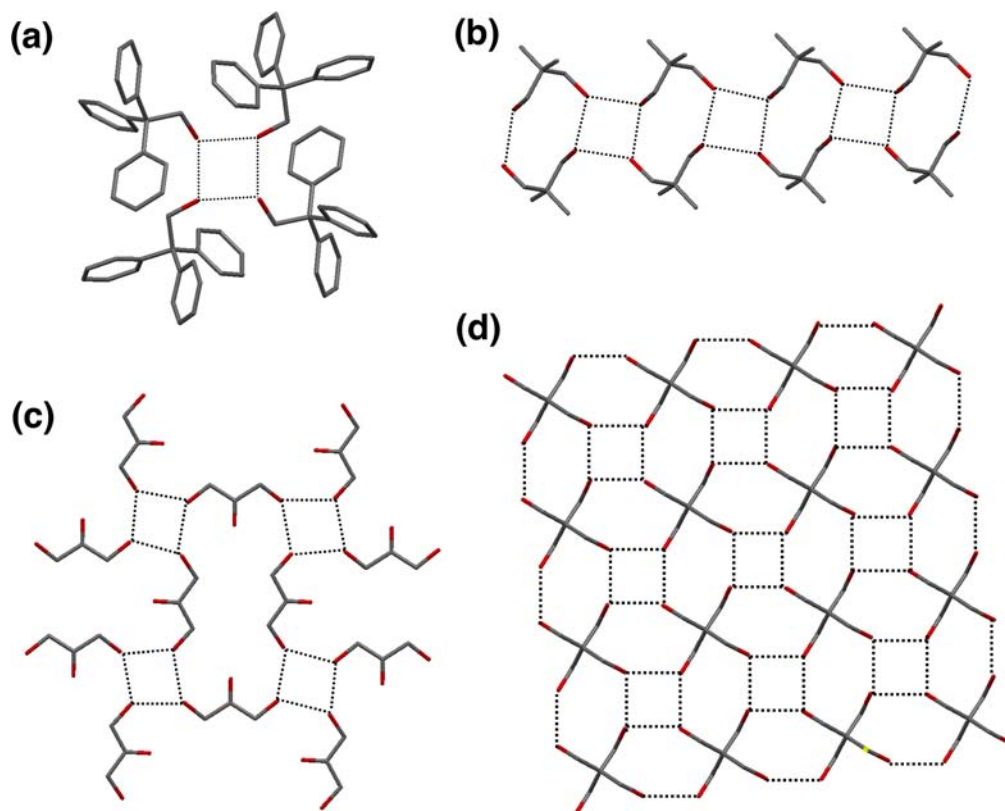


Figure 6. H-bonded cyclic tetramers found in X-ray crystal structures of alcohols in the CSD. Codes: (a) WERRUG, (b) NEPGCLO, (c) NADQZ, (d) PERYTO01.

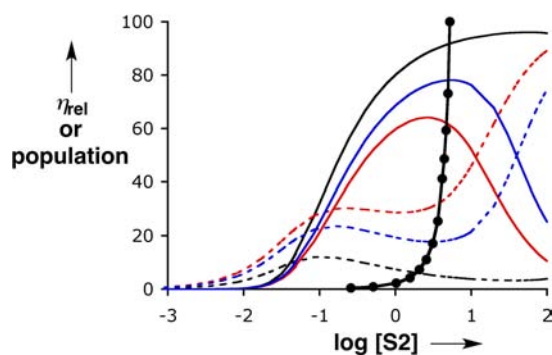


Figure 7. Relationship between the relative viscosity η_{rel} of *n*-decanol/*n*-heptane mixtures versus the logarithm of the concentration of *n*-decanol ($\log[S_2]$). The data points are the relative viscosity as defined by eq 3 expressed as a percentage. The solid lines are the calculated populations of *n*-decanol molecules present as cyclic tetramers, and the dotted lines are the calculated populations of *n*-decanol molecules present as linear oligomers expressed as percentages ($K_4 = 820 \text{ M}^{-3}$ and $K_n = 4 \text{ M}^{-1}$ red, $K_n = 3 \text{ M}^{-1}$ blue, $K_n = 2 \text{ M}^{-1}$ black).

the cyclic tetramer starts to appear at concentrations of about 0.1 M ($\log[S_2] = -1$), and this species is not associated with any significant change in viscosity. The black population curves in Figure 7 show that when a value of 2 M^{-1} is used for K_n , the tetramer predominates over the entire concentration range and open polymers are not formed to any significant extent. This is clearly inconsistent with the viscosity data. However, values of 3 or 4 M^{-1} for K_n give rise to substantial populations of linear polymer in the concentration range where the viscosity starts to increase (blue and red population curves in Figure 7). The NMR experiment is not sensitive to such small differences in

K_n , so we combine K_n from the viscosity data with K_4 from the NMR data to estimate the value of EM_4 for formation of the cyclic tetramer, which is of the order 1 M.

Solvent–Solute Interactions. Next we will examine the three component mixtures of two solvents, S1 and S2, and one of the solutes, either A or D. The association constants for the formation of 1:1 complexes of D with *n*-decanol, *n*-hexanoic acid, and 2-ethylhexyl acetamide in *n*-octane (K_D) were measured by UV–vis absorption titrations using D as the host and the polar solvent, S2, as the guest. The titration data fit well to a 1:1 binding isotherm in all cases, and the results are reported in Table 2. At high concentrations of S2, self-association of the polar solvent could compete with formation of the D·S2 complex, so the titration data were also fit to an isotherm that allowed for self-association of S2 using the self-association constants determined in the dilution experiments discussed above. The values of K_D^* determined in this way are very similar to the values obtained by fitting to a simple 1:1 isotherm, K_D . The reason is that D is much more polar than S2, and the D·S2 complex forms at concentrations at which S2 self-association is not significant.

The association constants for formation of 1:1 complexes of A with *n*-decanol, *n*-hexanoic acid, and 2-ethylhexyl acetamide in *n*-octane (K_A) were measured by ^{31}P NMR titrations using A as the host and S2 as the guest. The data fit well to a 1:1 binding isotherm in all cases, and the resulting values of K_A are reported in Table 2. The titration data were also fit to an isotherm that included self-association of S2 to give K_A^* , but these values are very similar to the values of K_A obtained by fitting to the simple 1:1 isotherm. The polarity of A means that the A·S2 complex is fully bound before S2 self-association becomes significant.

Table 2. Equilibrium Constants (M^{-1}) for Formation of the A·S2 and D·S2 Complexes Measured by UV–vis Absorption and ^{31}P NMR Titrations in *n*-Octane at 295 K^a

S2	α	β	experiment				eq 1	
			K_D	K_D^*	K_A	K_A^*	K_D	K_A
<i>n</i> -hexanoic acid	3.6	5.3	5 ± 2	11 ± 9	8300 ± 1500	8300 ± 200	50	2400
2-ethylhexyl acetamide	2.8	8.5	840 ± 50	830 ± 40	87 ± 9	130 ± 10	3800	100
<i>n</i> -decanol	2.7	5.3	30 ± 5	24 ± 5	35 ± 5	25 ± 5	98	70

^aExperimental values were obtained by fitting to isotherms that include S2 self-association (K_D^* and K_A^*) or omit S2 self-association (K_D and K_A), and calculated values were obtained using eq 1. All experiments were repeated at least twice and average values are quoted. The errors are twice the standard deviation. K_D refers to the interaction of S2 with 4-phenyl azophenol, and K_A refers to the interaction of S2 with tri-*n*-butyl phosphine oxide.

It is also possible to estimate values of K_D and K_A using eq 1 and the H-bond parameters for the functional groups involved.³⁷ The calculated values of K_D and K_A are within a factor of 4 of the experimental values. The results in Table 2 show that $K_A \gg K_D$ for *n*-hexanoic acid, so this solvent will solvate A more strongly than D. For 2-ethylhexyl acetamide, $K_A \ll K_D$, so this solvent will solvate D more strongly than A. For *n*-decanol, $K_A \approx K_D$, so the two solutes will be equally well solvated by S2 in this case.

Solute–Solute Interactions in Solvent Mixtures.

Association constants for formation of the A·D complex in *n*-octane/*n*-decanol, *n*-octane/*n*-hexanoic acid, and *n*-octane/2-ethylhexyl acetamide mixtures were measured using UV–vis titration experiments. When $\log K$ is between 2 and 5, this can be achieved using an automated UV–vis plate reader. However at high concentrations of the polar solvent S2, the association constant cannot be determined accurately by this method, so some manual titrations were also carried out. The titration data were fit to a 1:1 isotherm with a linear correction to account for the absorbance of A at higher guest concentrations, and the results are illustrated in Figure 8. Open circles represent data from individual binding experiments, filled circles represent averages of the experimental data over windows of 0.25 units on the $\log[S2]$ scale. Although the data are noisy, the general shapes of the $\log K$ versus $\log[S2]$ profiles are similar to Figure 4. For low S2 concentrations, the binding constant is the same as in pure *n*-octane. When the concentration of S2 is high enough, it starts to compete with S1 for solvation of the polar functional groups, and the binding constant starts to decrease with increasing concentrations of S2. The threshold values of $[S2]$ for the onset of preferential solvation are about 0.05 mM for *n*-hexanoic acid, 0.5 mM for 2-ethylhexyl acetamide, and 5 mM for *n*-decanol. The difference between the behavior of these systems and Figure 4 is that the gradient at high concentrations of S2 is not -1 : for *n*-hexanoic acid, the gradient is approximately -0.5 ; for 2-ethylhexyl acetamide, the gradient is approximately -1.5 ; and for *n*-decanol, the gradient is approximately -2 . These self-associating solvents not only have very different solvation properties from the non-self-associating organic solvents that we have studied previously^{14–16} but also are quite different from one another.

The values of K_D and K_A for interactions of D and A with S2 in S1 should provide some insight into the concentration of S2 at which preferential solvation by the more polar solvent takes place. The onset of preferential solvation of D by S2 should be at $\log[S2] = -\log K_D$, and similarly the onset of preferential solvation of A by S2 should be at $\log[S2] = -\log K_A$. These points are indicated by the vertical dashed lines in Figure 8. The change in gradient in Figure 8a is close to the point at which A

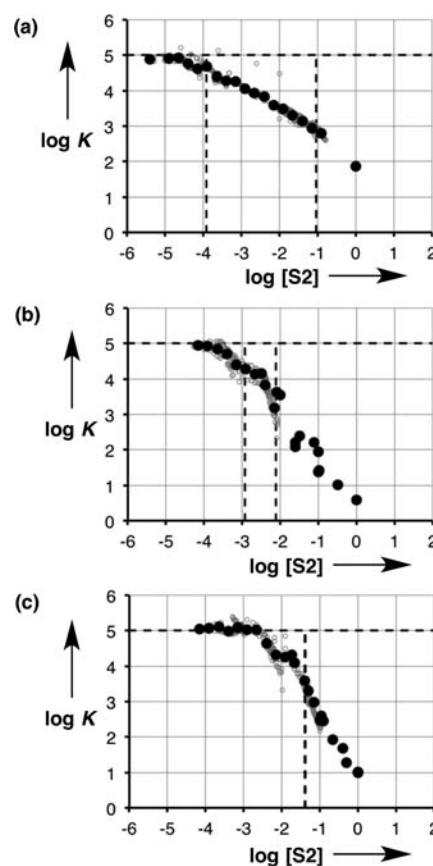


Figure 8. Association constant, K , for formation of the A·D complex in mixtures of *n*-octane (S1) and a more polar solvent, S2. (a) S2 = *n*-hexanoic acid. (b) S2 = 2-ethylhexyl acetamide. (c) S2 = *n*-decanol. Open circles represent data from individual binding experiments from automated titrations, and filled circles represent averages over a window of 0.25 units on the $\log[S2]$ scale. Data from manual titrations are shown as filled circles. The horizontal dotted line is plotted at $\log K = \log K_{S1}$. The vertical dotted lines are plotted at $\log[S2] = -\log K_D$ and $\log[S2] = -\log K_A$.

is solvated by S2, but the agreement is not so good in Figure 8b,c.

If we consider the pairwise interactions between A, D, and S2 that we have examined in the two and three component systems above, it should be possible to predict how the A·D association constant is expected to vary with the concentration of S2 in the four component system. The gray curves in Figure 9 shows the values of the A·D association constant calculated for dilute solutions of A and D ($1 \mu M$) in mixtures of S1 and S2 assuming that only the four equilibria illustrated in Figure 10 are important. In this model, only the S2 monomers solvate the

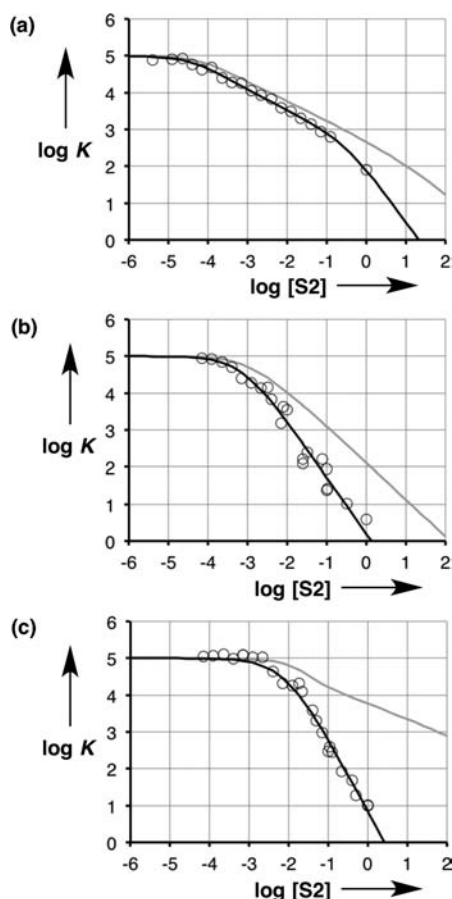


Figure 9. Association constant for formation of the A·D complex, K , in mixtures of *n*-octane and (a) *n*-hexanoic acid, (b) 2-ethylhexyl acetamide, and (c) *n*-decanol. Open circles represent the experimental data. The gray curves show $\log K$ calculated assuming that the solutes are solvated only by S2 monomers and not by S2 aggregates (Figure 10) and using the experimental values of K_{S1} , K_A , K_D , and K_{Sn} (where K_{Sn} is K_2 for *n*-hexanoic acid, K_n for 2-ethylhexyl acetamide and K_4 for *n*-decanol). The black curves show $\log K$ calculated assuming that the solutes are solvated by both S2 monomers and S2 aggregates (Figure 11) and by optimizing the values of K_A and K_D (the value of K_{Dn} was fixed at nK_D in all three cases, and the value of K_{An} was negligibly small in (a) and (b) and fixed at nK_A in (c)). $[A] = [D] = 1 \mu\text{M}$ in all calculations.

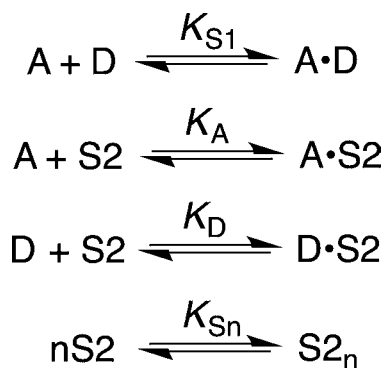


Figure 10. Equilibria in a four component mixture of two solutes, A and D, and two solvents, S1 and S2, where S1 is nonpolar and S2 self-associates. The S2 monomer solvates the solutes, but the S2 aggregate does not. Species like A·S2·D, where one molecule of S2 solvates two solutes, are not significantly populated at low solute concentrations.

solutes. The H-bond donor and acceptor sites in the S2 aggregates are assumed to be inaccessible, so that they do not solvate A or D, and self-association of S2 competes with solvation of the solutes. Although this model provides a reasonably good description of the experimental results for *n*-hexanoic acid (Figure 9a), the values of K are clearly overestimated at high concentrations of S2 in all three systems. This implies that both the S2 monomers and the S2 aggregates must play a role in solvating the solutes.

The calculated curves in Figure 9 are relatively sensitive to variations in the values used for K_A and K_D . We therefore used the experimental data in Figure 9 to obtain values of K_A and K_D that gave the best fit to the experimental data by optimizing these two parameters, while keeping the values of K_{S1} and K_n fixed at the experimentally determined values. In all three systems, the optimized values of K_A and K_D were more than an order of magnitude larger than the experimentally determined values in Table 2. This discrepancy is outside the experimental error and provides a clear indication that the S2 aggregates must play a role in solvating the solutes.

Figure 11 shows the set of equilibria that are required to adequately account for the experimental data. In this model,

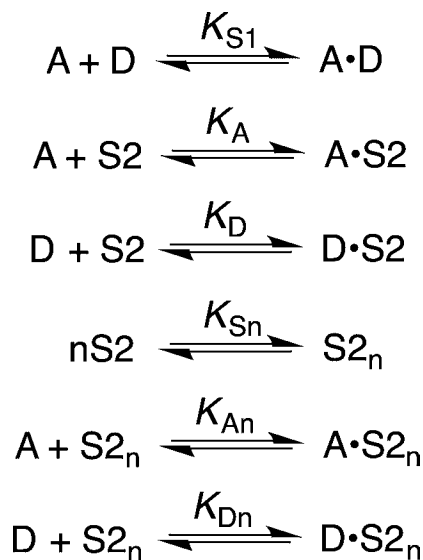


Figure 11. Equilibria in a four component mixture of two solutes, A and D, and two solvents, S1 and S2, where S1 is nonpolar and S2 self-associates. Both the S2 monomer and the S2 aggregate can solvate the solutes. Species like A·S2·D, where one molecule of S2 solvates two solutes, are not significantly populated at low solute concentrations.

both the S2 monomers and the S2 aggregates solvate the solutes, and this increases the effective polarity of the solvent at high S2 concentrations compared with the model in Figure 10. In all three types of S2 aggregate, the H-bond donor site on S2 is involved in an intermolecular H-bond with a H-bond acceptor site and so can be considered inaccessible for further interaction with solutes. However, the S2 aggregates all have additional H-bond acceptor sites that are not involved in intermolecular H-bonding interactions. The simplest description of the solvation properties of the S2 aggregates is therefore to assume that the H-bond acceptor sites interact with D with the same affinity as the equivalent H-bond acceptor sites on the S2 monomers, i.e. $K_{Dn} = nK_D$, where the statistical factor of n accounts for the number of H-bond acceptor sites in an *n*-mer.

The experimental data in Figure 9 were fit to the model in Figure 11 by optimizing the values of K_A and K_D with the values of K_{S1} and K_{S2} fixed at the experimental values, $K_{Dn} = nK_D$ and $K_{An} \ll 1 \text{ M}^{-1}$. The black curves in Figure 9a,b show that for *n*-hexanoic acid and 2-ethylhexyl acetamide, this provides good agreement with the experimental data for values of K_A and K_D that are comparable to the experimentally determined values (compare Tables 2 and 3). However, this is not the case for *n*-

Table 3. Equilibrium Constants (M^{-1}) for Formation of the A·S₂, A·S_{2n}, D·S₂, and D·S_{2n} Complexes in *n*-octane Obtained by Fitting the Experimental Values of K for Formation of the A·D Complex in S₁–S₂ Mixtures to the Model in Figure 11

S2	K_D	K_{Dn}	K_A	K_{An}
<i>n</i> -hexanoic acid	3	3	15 000	–
2-ethylhexyl acetamide	1500	1500	520	–
<i>n</i> -decanol	120	120	120	120

decanol, and in order to obtain good agreement with the experimental data for this system, it was necessary to include solvation of A by the S₂ aggregate. The black curve in Figure 9c shows the result of fitting the experimental data to the model in Figure 11 by optimizing the values of K_A and K_D with the values of K_{S1} and K_{S2} fixed at the experimental values, $K_{Dn} = nK_D$ and $K_{An} = nK_A$. The optimized values of K_A and K_D are comparable to the experimentally determined values (compare Tables 2 and 3).

These results imply that a H-bond donor that is interacting with a H-bond acceptor in an alcohol aggregate is readily able to form an additional bifurcated H-bond with a solute (Figure 12c).^{38,39} Moreover, the strength of this H-bond is comparable to the interaction with a monomeric alcohol. In contrast, bifurcated H-bonds are not required to account for the solvation properties of carboxylic acids or secondary amides. At high concentrations of S₂ (>1 M), aggregates are the predominant species for all three polar solvents, and Figure 12 illustrates the primary modes of solute solvation under these

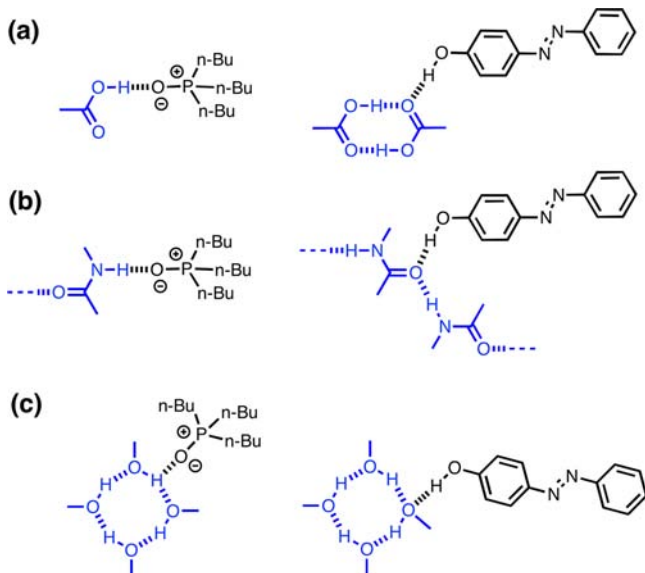


Figure 12. Primary modes of solvation for solutions of A and D in (a) *n*-hexanoic acid, (b) 2-ethylhexyl acetamide, and (c) *n*-decanol.

conditions. In all three solvents, H-bond donors are solvated primarily by aggregates. In acids, H-bond acceptors are solvated primarily by monomers. In amides, H-bond acceptors are solvated primarily by monomers or the ends of polymer chains. However in alcohols, H-bond acceptors are solvated primarily by bifurcated H-bonds to aggregates. This explains why alcohols show anomalously high polarity with respect to H-bond formation compared with other solvents.^{30,31}

The calculations described above provide a rationalization for the variation in the gradient of the log K versus log[S₂] profiles in Figure 9. In *n*-hexanoic acid, the gradient is -0.5 at the onset of preferential solvation by S₂. In this region where $0.1 \text{ mM} < [\text{S}_2] < 0.1 \text{ M}$, the concentration of S₂ is too low to solvate D but sufficiently high to solvate A and to form S₂ dimers. The S₂ dimer does not solvate A significantly, so solvation of A competes with dimerization of S₂. When $K_2[\text{S}_2] \gg 1$, S₂ is almost completely dimerized, and the concentration of S₂ monomer is $([\text{S}_2]/2K_2)^{1/2}$. Thus the concentration of S₂ monomer available to solvate A increases as the square root of the total concentration of S₂, and this gives rise to the slope of -0.5 in this region of the profile in Figure 9a. When $[\text{S}_2] > 1 \text{ M}$, the gradient of the log K versus log[S₂] profile in Figure 9a changes to -1.5 . In this region, the concentration of S₂ is sufficient to solvate D as well as A. Both the S₂ dimer and S₂ monomer solvate D with equal affinity, and so the contribution of solvation of D to the decrease in log K is linear in log[S₂]. The overall gradient in this region is therefore $-1.5:-0.5$ due to solvation of A plus -1 due solvation of D.

In 2-ethylhexyl acetamide, the gradient of the log K versus log[S₂] profile in Figure 9b is -1.5 after the onset of preferential solvation by S₂, i.e., for $[\text{S}_2] > 1 \text{ mM}$. The explanation is similar to that given above for *n*-hexanoic acid at high concentrations of S₂. When $[\text{S}_2] > 1 \text{ mM}$, the amide solvates both A and D. D is solvated equally by S₂ aggregates and S₂ monomers, and so the contribution of solvation of D to the decrease in log K is linear in log[S₂]. A is not significantly solvated by S₂ aggregates, and so the contribution of solvation of A to the decrease in K depends on the concentration of S₂ monomers. When S₂ is almost fully self-associated, the concentration of S₂ monomers increases as the square root of the total concentration of S₂. The overall gradient in this region is therefore $-1.5:-0.5$ due to solvation of A plus -1 due solvation of D.

In *n*-decanol, the gradient of the log K versus log[S₂] profile in Figure 9c is -2 after the onset of preferential solvation by S₂, i.e. for $[\text{S}_2] > 10 \text{ mM}$. In this region, the S₂ aggregates and S₂ monomers solvate A and D equally well. Thus the contribution of solvation of D to the decrease in log K is linear in log[S₂], and the contribution of solvation of A to the decrease in log K is linear in log[S₂]. The overall gradient in this region is therefore $-2:-1$ due to solvation of A plus -1 due solvation of D.

These results suggest that alcohol solvents should show anomalously high polarity, which is consistent with our previous observations but inconsistent with Abraham's measurements of H-bond association constants in *n*-octanol using headspace gas liquid chromatography.³² We have therefore selected some of the high affinity complexes from this work and measured the association constant by ³¹P NMR titrations in *n*-octanol. NMR titrations were carried out using three H-bond donors, 2,2,2-trifluoroethanol, hexafluoro-*i*-propanol and perfluoro-*t*-butanol, and two H-bond acceptors, triethyl phosphate and tri-*n*-butyl phosphine oxide. In all six

cases, the binding constants were very low, and the guest had to be added as a pure liquid to obtain a binding isotherm. Although the association constants were too low to be measured accurately, and the values obtained from the NMR titrations ($K < 1 \text{ M}^{-1}$) are clearly much lower than the values measured by headspace gas liquid chromatography. For example, Figure 13 compares the ^{31}P NMR titration data

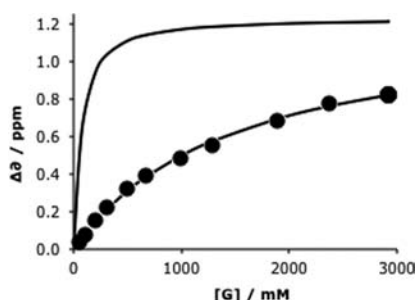


Figure 13. Change in chemical shift measured in a ^{31}P NMR titration between triethyl phosphate (50 mM) and perfluoro-*t*-butanol in *n*-octanol at 295 K. The line through the data points is the best fit to a 1:1 binding isotherm ($\log K/\text{M}^{-1} = -0.16$). The other line is the isotherm calculated using $\log K/\text{M}^{-1} = 1.30$ as measured by Abraham.

recorded in *n*-octanol for the perfluoro-*t*-butanol-triethyl phosphate complex with the corresponding isotherm calculated using the association constant measured by Abraham ($K = 20 \text{ M}^{-1}$).³² There is clearly a significant discrepancy between the behavior of these systems when studied using solution NMR and head space gas liquid chromatography.

CONCLUSIONS

Studies of H-bonding interactions between polar solutes in mixtures of alkanes and polar solvents provide insight into the solvation properties of complex systems. Carboxylic acids, secondary amides, and alcohols are solvents where self-association is extensive in the bulk liquid leading to complex solvation environments. Dilution studies in alkanes have allowed us to characterize the aggregates formed by three self-associating solvents: carboxylic acids form dimers, secondary amides form linear polymers, and alcohols form both linear and cyclic aggregates. These self-associated species have surprisingly different effects on the solvation of solutes. In all three cases, solvent aggregates and solvent monomers interact with H-bond donor solutes with a similar binding affinity. The reason is that all three solvents have two identical H-bond acceptor sites: formation of aggregates blocks one site but leaves the second site exposed for further interaction with solutes. In carboxylic acid dimers and secondary amide polymeric aggregates, the solvent H-bond donor sites are buried and do not contribute to solvation of H-bond acceptor solutes. However, our experiments show that alcohol aggregates solvate H-bond acceptor solutes with a similar binding affinity to alcohol monomers. This implies that alcohol H-bond donor sites are sufficiently exposed in solvent aggregates to make bifurcated H-bonds with solutes and that these interactions are similar in strength to conventional H-bonds. As a result, alcohols are significantly more polar solvents than might be expected based on the properties of monomers in dilute solutions.

EXPERIMENTAL SECTION

All solvents were HPLC grade and were used without further purification, apart from 2-ethylhexyl acetamide. The synthesis and purification of this solvent is described below. The plates used in the titration experiments on the plate reader are not sealed, and the possible effects of absorption of water from the atmosphere were not investigated. All other chemicals used were purchased from Aldrich and used without further purification. Tri-*n*-butyl phosphine oxide was dried in a vacuum desiccator over phosphorus pentoxide before use. Calculations to generate Figure 9, i.e., speciation in multi-component equilibria, were carried out using Microsoft Excel macros.

Automated UV-vis Titrations. Association constants were determined using a BMG Labtech Fluorostar Optima plate reader with a Hellma 96-well quartz microplate. In a typical experiment, the microplate contained two titrations: the first in *n*-octane (S1) in wells 1–48 and the second in *n*-decanol, *n*-hexanoic acid, or 2-ethylhexyl acetamide (S2) in wells 49–96. In addition to mixtures of pure solvents, dilute solutions of the solvent of interest dissolved in *n*-octane were also used as S2. These solvent mixtures were prepared by volume, apart from mixtures of *n*-octane and 2-ethylhexylacetamide, which is a viscous oil, and so was transferred by mass. For example, a 2% vol solution of *n*-decanol in *n*-octane was prepared by transferring 2 mL of *n*-decanol to a 100 mL volumetric flask, and the flask was then filled with *n*-octane.

Manual UV-vis Titrations. Manual titrations were carried out using a Cary 3 Bio UV-vis spectrophotometer. A 4 mL sample of the host (D) was prepared at a known concentration ($\approx 0.02 \text{ mM}$). 0.7 mL of this solution was removed and added to a 1 mL quartz cuvette, and the UV-vis spectrum was recorded. The guest (S2 or A) was then dissolved in the remaining host solution to avoid dilution of the host during the titration. The choice of concentration of the guest stock solution is based on the stability of the complex ($[G] \approx 20/K$). Aliquots of guest solution were added successively to the cuvette containing the host solution, the cuvette was shaken, and the UV-vis absorption spectrum was recorded after each addition. The observed changes in UV-vis absorption were fit to a 1:1 binding isotherm using Microsoft Excel.

NMR Titration Experiments. ^{31}P NMR titrations were carried out using a Bruker Avance III 400 spectrometer. A 4 mL sample of the host (A) was prepared at a known concentration (0.1–10 mM). 0.5 mL of this solution was removed, and a ^{31}P NMR spectrum was recorded using an external capillary containing a 5 mM solution of methylene diphosphonic acid in D_2O to provide a ^{31}P reference signal (17.98 ppm) and a deuterium lock signal. The guest (S2) was then dissolved in the remaining host solution to avoid dilution of the host during the course of the experiment. The concentration of S2 varied depending on the stability of the A-S2 complex ($[S2] \approx 20/K$). Aliquots of guest solution were added successively to the NMR tube containing the host solution, the tube was shaken thoroughly, and the ^{31}P NMR spectrum was recorded after each addition. The observed changes in chemical shift were fit to a 1:1 binding isotherm using Microsoft Excel.

NMR Dilution Experiments. ^1H NMR dilutions were carried out using a Bruker Avance III 400 spectrometer. 0.6 mL of d_{12} -cyclohexane was placed in an NMR tube. A 3 mL sample of S2 in d_{12} -cyclohexane was prepared at a known concentration. Aliquots of the S2 solution were added to the NMR tube, the tube was shaken thoroughly, and the ^1H NMR spectrum was recorded after each addition. The observed changes in chemical shift were fit to various isotherms using Microsoft Excel.

Synthesis of 2-Ethylhexyl Acetamide. Triethylamine (41.2 g, 0.408 mol) was added to a stirred solution of 2-ethylhexylamine (45.2 g, 0.350 mol) in dichloromethane (1 L) under nitrogen. Acetyl chloride (31.8 g, 0.408 M) was added to the reaction mixture via a pressure equalizing dropping funnel. After 4 h, the reaction was quenched with 1 L of sodium hydroxide (10% solution), extracted with dichloromethane ($5 \times 200 \text{ mL}$) and then washed with 1 L of brine. The organic layer was dried over sodium sulfate, filtered, and concentrated *in vacuo* to give a pale-yellow oil. The crude product was

purified on a charcoal-silica column eluting with dichloromethane/ethyl acetate, followed by a reduced pressure distillation (b.p. 100–110 °C at 13 mbar) to yield a clear oil (31.1 g, 52%). ¹H NMR (400 MHz, CDCl₃): δ 6.45 (br s, 1H), 3.08 (m, 2H), 1.91 (s, 3H), 1.39 (m, 1H), 1.25 (m, 8H), 0.85 (m, 6H). ¹³C NMR (100.6 MHz, CDCl₃): δ 170.43, 42.48, 39.18, 30.84, 28.78, 24.02, 23.08, 22.94, 13.98, 10.69. TOF MS ES+: *m/z* (%) = 172 (100) [M – H⁺].

■ ASSOCIATED CONTENT

■ Supporting Information

Equations used in analysis of the binding isotherms and representative titration data. This material is available free of charge via the Internet at <http://pubs.acs.org>.

■ AUTHOR INFORMATION

Corresponding Author

c.hunter@sheffield.ac.uk

Notes

The authors declare no competing financial interest.

■ ACKNOWLEDGMENTS

We thank the EPSRC for financial support.

■ REFERENCES

- (1) Reichardt, C. In *Solvents and Solvent Effects in Organic Chemistry*; Wiley-VCH: Weinheim, 2003.
- (2) Marcus, Y. In *The Properties of Solvents*; Wiley: Chichester, 1998.
- (3) Ben-Naim, A. In *Solvation Thermodynamics*; Plenum Press: New York, 1987.
- (4) Abrams, D. S.; Prausnitz, J. M. *AIChE J.* **1975**, *21*, 116.
- (5) Symons, M. C. R.; Fletcher, N. J.; Thompson, V. *Chem. Phys. Lett.* **1979**, *60*, 323–325.
- (6) Symons, M. C. R.; Harvey, J. M.; Jackson, S. E. *J. Chem. Soc. Faraday I* **1980**, *76*, 256–265.
- (7) Barker, J. A.; Henderson, D. *Rev. Mod. Phys.* **1976**, *48*, 587–671.
- (8) Marten, B.; Kim, K.; Cortis, C.; Friesner, R. A.; Murphy, R. B.; Ringnalda, M. N.; Sitkoff, D.; Honig, B. *J. Phys. Chem.* **1996**, *100*, 11775–11788.
- (9) Handgraaf, J.-W.; Meijer, E. J.; Gageot, M.-P. *J. Chem. Phys.* **2004**, *121*, 10111–10119.
- (10) Lee, H.-S.; Tuckerman, M. E. *J. Phys. Chem.* **2006**, *125*, 154507.
- (11) Chapman, W. G.; Gubbins, K. E.; Jackson, G.; Radosz, M. *Ind. Eng. Chem. Res.* **1990**, *29*, 1709–1721.
- (12) Klamt, A. *J. Phys. Chem.* **1995**, *99*, 2224–2235.
- (13) Klamt, A.; Eckert, F. *Fluid Phase Equilib.* **2000**, *172*, 43–72.
- (14) Buurma, N. J.; Cook, J. L.; Hunter, C. A.; Low, C. M. R.; Vinter, J. G. *Chem. Sci.* **2010**, *1*, 242–246.
- (15) Amenta, V.; Cook, J. L.; Hunter, C. A.; Low, C. M. R.; Vinter, J. G. *Org. Biomol. Chem.* **2011**, *9*, 7571–7578.
- (16) Amenta, V.; Cook, J. L.; Hunter, C. A.; Low, C. M. R.; Vinter, J. G. *J. Phys. Chem. B* **2012**, *116*, 14433–14440.
- (17) Martin, A. E. *Nature* **1950**, *166*, 474–475.
- (18) Abraham, M. H.; Duce, P. P.; Schulz, R. A.; Morris, J. J.; Taylor, P. J.; Barratt, D. G. *J. Chem. Soc. Faraday, Trans. I* **1986**, *82*, 3501–3514.
- (19) Laplanche, L. A.; Rogers, M. T. *J. Am. Chem. Soc.* **1964**, *86*, 337–341.
- (20) Mizushima, S. I.; Simanouti, T.; Nagakura, S.; Kuratani, K.; Tsuboi, M.; Baba, H.; Fujioka, O. *J. Am. Chem. Soc.* **1950**, *72*, 3490–3494.
- (21) Suzuki, I. *Bull. Chem. Soc. Jpn.* **1962**, *35*, 540–551.
- (22) Russell, R. A.; Thompson, H. W. *Spectrochim. Acta* **1956**, *8*, 138–141.
- (23) Degraaf, D. E.; Sutherland, G. *J. Chem. Phys.* **1957**, *26*, 716–717.
- (24) Leader, G. R.; Gormley, J. F. *J. Am. Chem. Soc.* **1951**, *73*, 5731–5733.
- (25) Davies, M.; Thomas, D. K. *J. Phys. Chem.* **1956**, *60*, 41–44.

- (26) Saunders, M.; Hyne, J. B. *J. Chem. Phys.* **1958**, *29*, 1319–1323.
- (27) Saunders, M.; Hyne, J. B. *J. Chem. Phys.* **1958**, *29*, 253–254.
- (28) Costas, M.; Patterson, D. *J. Chem. Soc., Faraday Trans. I* **1985**, *81*, 635–654.
- (29) Karachewski, A. M.; McNeil, M. M.; Eckert, C. A. *Ind. Eng. Chem. Res.* **1989**, *28*, 315–324.
- (30) Frange, B.; Abboud, J. L. M.; Benamou, C.; Bellon, L. *J. Org. Chem.* **1982**, *47*, 4553–4557.
- (31) Cook, J. L.; Hunter, C. A.; Low, C. M. R.; Perez-Velasco, A.; Vinter, J. G. *Angew. Chem., Int. Ed.* **2007**, *46*, 3706–3709.
- (32) Abraham, M. H.; Gola, J. M. R.; Cometto-Muniz, J. E.; Acree, W. E. *J. Org. Chem.* **2010**, *75*, 7651–7658.
- (33) Martinez, A. G.; Vilar, E. T.; Fraile, A. G.; Martinez-Ruiz, P. *J. Chem. Phys.* **2006**, *124*, 234305.
- (34) Cabot, R.; Hunter, C. A.; Varley, L. M. *Org. Biomol. Chem.* **2010**, *8*, 1455–1462.
- (35) Brock, C. P.; Duncan, L. L. *Chem. Mater.* **1994**, *6*, 1307–1312.
- (36) Sastry, N. V.; Valand, M. K. *J. Chem. Eng. Data* **1996**, *41*, 1426–1428.
- (37) Hunter, C. A. *Angew. Chem., Int. Ed.* **2004**, *43*, 5310.
- (38) Rozas, I.; Alkorta, I.; Elguero, J. *J. Phys. Chem. A* **1998**, *102*, 9925–9932.
- (39) Etter, M. C. *Acc. Chem. Res.* **1990**, *23*, 120–126.